Logarithmic, noise-induced dynamics in the Anderson insulator

Talía L. M. Lezama[1] and Yevgeny Bar Lev[1]

[1] *Department of Physics, Ben-Gurion University of the Negev, Beer-Sheva 84105, Israel*

We study the dynamical behavior of the one-dimensional Anderson insulator in the presence of a local noise. We show that the noise induces logarithmically slow energy and entanglement growth, until the system reaches an infinite-temperature state, where both quantities saturate to extensive values. The saturation value of the entanglement entropy approaches the average entanglement entropy over all possible product states. At infinite temperature, we find that a density excitation spreads logarithmically with time, without any signs of asymptotic diffusive behavior. In addition, we provide a theoretical picture which qualitatively reproduces the phenomenology of particle transport.

I. INTRODUCTION

Anderson localization is an ubiquitous wave phenomenon that arises due to destructive interference in the presence of quenched disorder [1]. Since its discovery, it has been instrumental for the understanding of a much richer class of physical phenomena [2–6]. One of the most important manifestations of Anderson localization is the suppression of transport which follows from the exponential localization of all the single-particle wavefunctions in one and two dimensions [1, 7], such that infinitesimally small disorder leads to zero DC-conductivity at any temperature. While in higher dimensions, and at zero temperature, a metal-insulator transition takes place [7]. The phenomenon of Anderson localization has been extensively studied [8, 9], and experimentally demonstrated in many systems [10–17]. Even if most of the experimental setups are highly controlled, it is impossible to completely isolate the system from all dissipation effects that arise due to the coupling to the environment, for example, coupling to phonons is present in any condensed matter system, and is known to induce a finite DC conductivity [18]. It is therefore of importance to theoretically account for such dissipative processes.

The stability of Anderson localization to different classes of perturbations has been assessed in several theoretical studies [4–6, 19–28]. Anderson localization is known to be stable under spatially local but quasiperiodic in time perturbations in any dimension [20], and to survive global periodic driving in one dimension [27, 29]. In contrast, it is unstable to global noise, which is known to induce delocalization [22, 23, 26, 28, 30–34], and a transient subdiffusive transport, which eventually crosses over to regular diffusion [26, 34]. Global noise was also shown to lead to prethermal energy plateaus at intermediate time scales, followed by exponential relaxation at longer time scales [28]. The stability of localized systems has also been studied extensively in recent experiments with ultracold atoms in optical lattices [35–37] .

In this work, we study how the dynamics in the one-dimensional Anderson insulator is affected by the presence of a *local* white-noise, which can be thought as a coupling to a local Markovian bath. We find that the noise leads to a logarithmically slow heating of the system up to an infinite-temperature state which is further reflected in slow transport properties of the system.

Our article is organized as follows. In Sec. II, we introduce the model and the methods used to characterize the noise-induced dynamics. In Sec. III, we first assess the heating dynamics in terms of the energy and the entanglement entropy. We then analyze the particle transport in the system using both numerical simulations and a semi-analytical approach. In Sec. V, we summarize and discuss our main results.

II. MODEL AND METHODS

We consider the one-dimensional Anderson model,

$$\hat{H}_A = -J\sum_{i=1}^{L-1}\left(\hat{c}_i^\dagger \hat{c}_{i+1} + \text{h.c.}\right) + \sum_{i=1}^{L} w_i \hat{n}_i, \tag{1}$$

where $\hat{c}_i^\dagger$ ($\hat{c}_i$) creates (annihilates) a spinless electron on site i, "h.c." stands for a Hermitian conjugate, $\hat{n}_i = \hat{c}_i^\dagger \hat{c}_i$ is the density, and J denotes the hopping constant. The on-site disorder potential, w_i, are independent random variables uniformly distributed in the interval $w_i \in [-W, W]$, with W the disorder strength. This model is known to be localized

for any $W > 0$ [1]. We perturb the Anderson model, by the addition of a local white-noise,

$$\hat{H} = \hat{H}_A + \zeta(t)\,\hat{n}_{L/2}, \tag{2}$$

such that $\zeta(t)$ has zero mean $\overline{\zeta(t)} = 0$ and a vanishing correlation length

$$\overline{\zeta(t)\,\zeta(t')} = \gamma\delta(t-t'), \tag{3}$$

where the overbar denotes the average over stochastic realizations of the noise and γ is the noise strength. The noise term represents a local Markovian heat bath coupled to the system, and as such, the dynamics of the density matrix of the system, $\hat{\rho}(t)$, is given by the following Lindblad equation [38]

$$\begin{aligned}\partial_t\hat{\rho}(t) = &-i\left[\hat{H}_A, \hat{\rho}(t)\right] + \\ &+\gamma\Big(\hat{n}_{L/2}\hat{\rho}(t)\,\hat{n}_{L/2} - \frac{1}{2}\left\{\hat{n}_{L/2}, \hat{\rho}(t)\right\}\Big),\end{aligned} \tag{4}$$

where $\{\cdot,\cdot\}$ is the anti-commutator. The Lindblad equation describes a trace-preserving non-unitary evolution, where the first term corresponds to the unitary evolution, and the second term corresponds to the dissipative coupling between the system and the local heat bath. It is easy to check by substitution, that the steady state of (4) is an infinite-temperature state with density matrix $\hat{\rho}_\infty \propto \mathbb{1}$, which means that for any initial state the system will approach $\hat{\rho}_\infty$. Please note, that the approach to infinite temperature by itself does *not* imply delocalization of the system, since as stated above, in one and two dimensions, and without the coupling to the noise, localization persists also at infinite temperature [1]. Here, we focus on the questions of *how* the infinite-temperature state is approached and what is the dynamics of the system at this state, in the presence of a local noise.

While (4) can be numerically solved, this is extremely demanding even for noninteracting particles, since certain couplings to the heat bath create an effective interaction between the particles, which requires the use of the full many-body density matrix of dimensions $\mathcal{N}\times\mathcal{N}$, where $\mathcal{N}$ is the Hilbert-space dimension. Alternative methods, based on a unitary propagation followed by stochastic measurements, of an ensemble of wavefunctions, were developed [39–43]. These methods, known as quantum-trajectory methods, are more efficient since the dimension of the wavefunction is $\mathcal{N}$. The solution of (4) is reproduced by an average over quantum trajectories, which correspond to individual realizations of the measurements. The procedure of writing (4) as a stochastic differential equation, is known as "unraveling", and since there can be many stochastic differential equations whose averages reproduce (4), the procedure is not unique, and can depend on the physical context [41].

In this work, we use a unitary unraveling of (4), which was introduced in Refs. [42, 43] and corresponds to the following stochastic unitary infinitesimal propagator

$$\hat{U}(t+\mathrm{d}t, t) = e^{-i\hat{H}\mathrm{d}t - i\eta_t\hat{n}_{L/2}\sqrt{\gamma dt}}, \tag{5}$$

where η_t are independent normally distributed random variables of zero mean and unit variance. The evolution of the density matrix is then obtained by performing an average over trajectories corresponding to the different realizations of the noise η_t, namely,

$$\hat{\rho}(t+\mathrm{d}t) = \overline{|\psi(t+\mathrm{d}t)\rangle\langle\psi(t+\mathrm{d}t)|}, \tag{6}$$

where the overbar denotes the average over the noise trajectories, and $|\psi(t+\mathrm{d}t)\rangle = \hat{U}(t+\mathrm{d}t, t)\,|\psi(t)\rangle$, with the initial condition $|\psi(t=0)\rangle$ taken from an ensemble whose average corresponds to the initial density matrix $\hat{\rho}(t=0) = \overline{|\psi(t=0)\rangle\langle\psi(t=0)|}$.

For self-adjoint Lindblad operators this unraveling is equivalent to the quantum-jump approach [43], but is numerically superior for an initial quadratic density matrix $\hat{\rho}(t=0) = e^{-\sum_i \alpha_i\hat{n}_i}$, since it only requires the propagation of a *single-particle* density matrix

$$\rho^s_{ij}(t) \equiv \mathrm{Tr}\left(\hat{\rho}(t)\;\hat{c}_i^\dagger\hat{c}_j\right), \tag{7}$$

which is polynomial rather than exponential in L. This simplification occurs, since $\hat{U}(t+\mathrm{d}t, t)$ is quadratic in $\hat{c}_i^\dagger$ ($\hat{c}_i$) and therefore an initially quadratic density matrix, stays quadratic for the entire evolution of the system. The propagation of $\rho^s_{ij}(t)$ is obtained using the single-particle version of the stochastic unitary propagator (5),

$$U^s(t+\mathrm{d}t, t) = e^{-i\hat{h}_A\mathrm{d}t - i\eta_t|L/2\rangle\langle L/2|\sqrt{\gamma dt}}, \tag{8}$$

where

$$\hat{h}_A = -J \sum_{i=1}^{L-1} \left(|i\rangle \langle i+1| + |i+1\rangle \langle i| \right) + \sum_{i=1}^{L} w_i |i\rangle \langle i| \tag{9}$$

is the single-particle Anderson Hamiltonian. The evolved single-particle density matrix $\rho^s_{ij}(t + \mathrm{d}t)$ is therefore given by,

$$\rho^s_{ij}(t + \mathrm{d}t) = \overline{U^s_{ik}(t + \mathrm{d}t, t)\, \rho^s_{kl}(t)\, \hat{U}^{s*}_{jl}(t + \mathrm{d}t, t)}. \tag{10}$$

For our numerical simulations we use Krylov-space methods and time steps of $dt = 0.1$, although the unraveling we use is exact for any dt. We fix the tunneling constant to $J = 1$, which determines the units of time and set the noise strength to $\gamma = 1$; changing the amplitude of the noise, does not change our results qualitatively. We average our results over 100 disorder realizations and 10 realizations of the noise for each disorder realization, which we verified to be sufficient to obtain converged results. The averages over disorder and over noise are denoted by square brackets $[\cdot]$ and by an overbar $\bar{\cdot}$, respectively.

III. RESULTS

In this section we characterize how the system approaches an infinite-temperature state in terms of the energy and a properly defined entanglement entropy. We then assess the linear response particle transport at infinite temperature.

A. Energy dissipation

The energy of the system,

$$\varepsilon(t) = \mathrm{Tr}\left(\hat{\rho}(t)\, \hat{H}_A \right), \tag{11}$$

grows as a result of coupling to the local heat bath. Since $\hat{H}_A = \sum_{ij} \left\langle i \left| \hat{h}_A \right| j \right\rangle \hat{c}^\dagger_i \hat{c}_j$, we can express the energy growth using the single-particle density matrix as,

$$\begin{aligned} \varepsilon(t) &= \sum_{i,j} \left\langle i \left| \hat{h}_A \right| j \right\rangle \mathrm{Tr}\left(\hat{\rho}(t)\, \hat{c}^\dagger_i \hat{c}_j \right) \\ &= \sum_{i,j} \rho^s_{ij}(t) \left\langle i \left| \hat{h}_A \right| j \right\rangle, \end{aligned} \tag{12}$$

where $|i\rangle$ and $|j\rangle$ are single-particle states in the position basis. Following the discussion of Sec. II, at long times, the system approaches an infinite-temperature state, $\hat{\rho}_\infty \propto \mathbb{1}$, therefore,

$$\varepsilon(t \to \infty) = \frac{1}{\mathcal{N}} \mathrm{Tr}\left(\hat{H}_A \right) = \frac{1}{2} \mathrm{Tr}\, \hat{h}_A = \frac{1}{2} \sum_i^L w_i, \tag{13}$$

where $\mathcal{N}$ is the Hilbert space dimension. Since the energy of the system is bounded, to have a sufficiently wide range of energy growth, we prepare the system in the ground state of $\hat{H}_A$. In this state, the single-particle density matrix is given by,

$$\rho^s_{ij}(0) = \sum_{\alpha=1}^{N} \phi^*_\alpha(i)\, \phi_\alpha(j), \tag{14}$$

where $\phi_\alpha(i) \equiv \langle i | \alpha \rangle$ are single-particle eigenstates of $\hat{h}_A$ ordered by energy, and N is the number of fermions, which we set to be $N = L/2$, namely, half-filling.

In Fig. 1(a) we show how the averaged (over realizations of disorder and trajectories) energy absorbed from the coupling to the local environment, $\Delta\varepsilon(t) = \left[\overline{\varepsilon(t) - \varepsilon_{\mathrm{GS}}} \right]$, grows in time for several disorder strengths W and a fixed

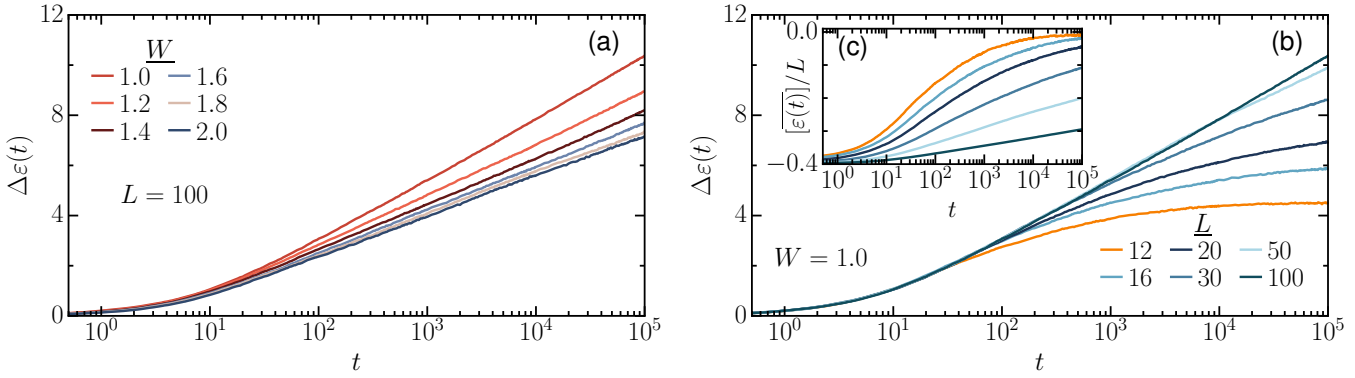

Figure 1. Averaged energy logarithmic growth starting from the ground state of the Anderson model. (a) As a function of disorder strength W for a system size $L = 100$.(b) As a function of system size L for $W = 1.0$.(c) Inset showing the saturation of the energy density $[\overline{\varepsilon(t)}]/L$ to an infinite-temperature state at long times for the smaller system sizes.

system size $L = 100$. We observe that the averaged absorbed energy grows logarithmically with time, $\Delta\varepsilon \sim \ln t$, over a broad time window extending into several decades and for all the disorder strengths we study. Increasing the disorder strength further suppresses the heating. Interestingly, this logarithmically slow energy growth resembles the heating in a vicinity of the Floquet-MBL transition [44].

In Fig. 1(b), we show how $\Delta\varepsilon\,(t)$ depends on system size L, for a weak disorder $W = 1$. For the smallest system size $L = 12$, the absorbed energy saturates, but as we increase the system size, the times required to observe saturation significantly increase. Since the energy of the system is extensive, to compare the saturation of the energy for different system sizes we calculate the energy density $\varepsilon(t)/L$. The results are presented in the inset of Fig. 1(b) and show the approach to an energy density corresponding to an infinite-temperature state, which for $\hat{H}_A$ is $\varepsilon_\infty/L = \frac{1}{2}\langle w_i\rangle = 0$.

B. Entanglement entropy growth

The entanglement entropy is not a good entanglement measure for mixed states [45], and therefore is not a natural quantity to consider for dissipative dynamics given by (4). While one can calculate the time-dependent entanglement for each of the unraveled pure states, since the entanglement entropy is not a linear function of the wavefunctions, the averaged entanglement entropies corresponding to different unravelings of (4) do *not* need to coincide (see [46] and references therein). Notwithstanding, if a certain unraveling can be justified by an underlying physical process, the use of such an averaged entanglement acquires physical meaning, and has implications on spread of correlations and transport [40]. Specifically, the unitary unraveling of Refs. [42, 43] that we use here, is applicable to systems attached to a local time-dependent potential, with a frequency band-width much larger than any other energy scale. For such systems, the computed average entanglement entropy bounds transport or correlations spreading in the system, and therefore, any dynamics can go faster than the entanglement dynamics.

To calculate the von-Neumann entanglement entropy we partition the system into two spatially equal parts A and B. For noninteracting systems the entanglement between A and B is given by [47]

$$S\,(t) = -\sum_{\alpha}\Big[\tilde{n}^A_\alpha\,(t)\log\tilde{n}^A_\alpha\,(t) + \big(1-\tilde{n}^A_\alpha\,(t)\big)\log\big(1-\tilde{n}^A_\alpha\,(t)\big)\Big], \tag{15}$$

where $\tilde{n}^A_\alpha\,(t)$ are the eigenvalues of the single-particle density matrix $\rho^s_{ij}\,(t)$ with $i,j \in A$. To have a sizable regime of entanglement growth we initiate the system at a random product state, namely, $\rho^s_{ij}\,(t=0) = n_j\delta_{ij}$, with random $n_j \in \{0,1\}$.

In Fig. 2(a), we show the time evolution of the entanglement entropy $S\,(t)$, averaged over disorder and trajectories realizations, for various disorder strengths W, and a fixed system size $L = 100$. Similar to the energy, we find that the averaged entropy grows logarithmically with time and that the slope of its growth is suppressed with disorder strength. Since the entanglement is bounded, the growth saturates at long times to $S_\infty \equiv \lim_{t\to\infty} S\,(t)$, as is apparent for the smaller system sizes in Fig. 2(b). The entanglement entropy density $S\,(t)\,/L$, for different system sizes approaches

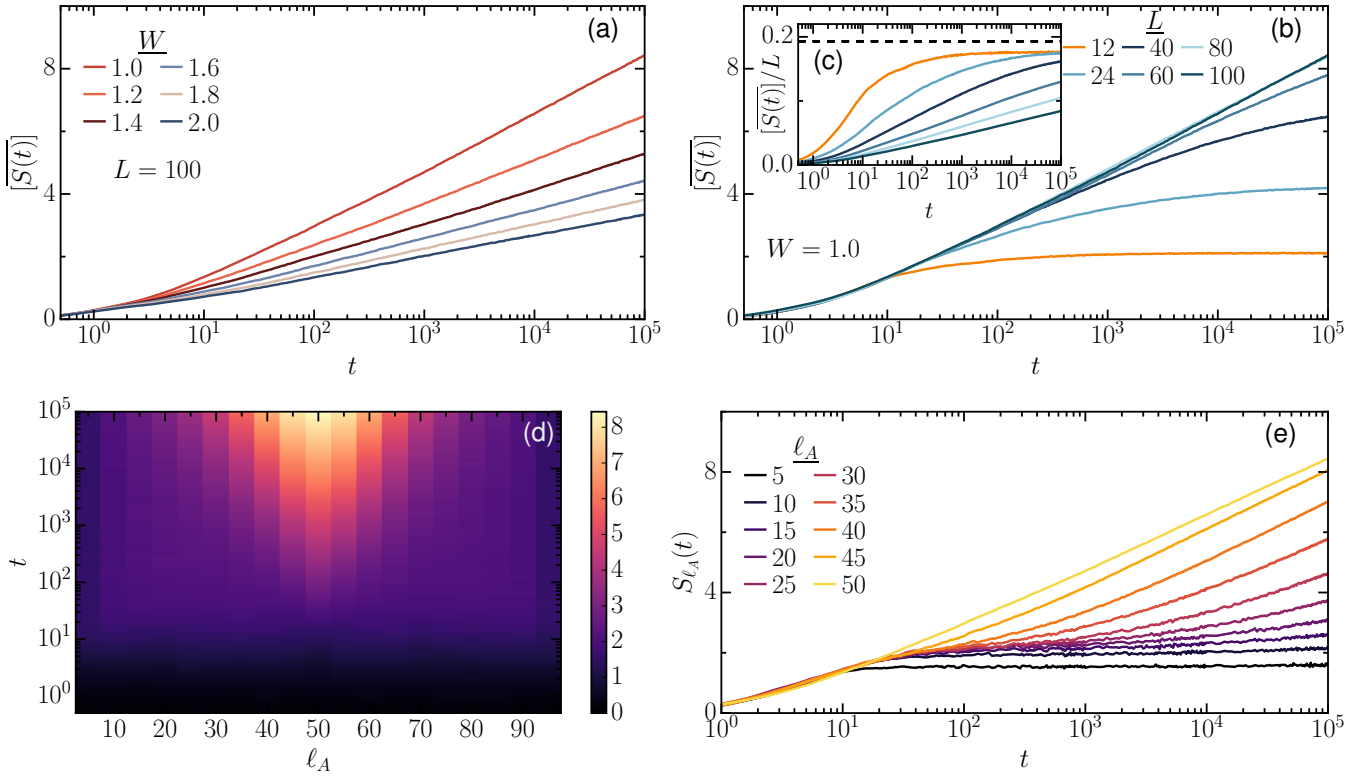

Figure 2. Upper panels: Logarithmic entanglement growth starting from random product states. (a) As a function of disorder strength W for $L = 100$, and (b) as a function of system size L for $W = 1.0$. (c) Inset showing the saturation of the averaged entanglement entropy density for the smaller system sizes and diverging exponentially with increasing system size. The dashed line in (c) refers to the entanglement entropy density averaged over all possible product states, $\bar{\mathcal{S}}/L \approx 0.193$ (see Eq. (2) in Ref. [50]). Lower panels: Entanglement profile. (d) Entanglement entropy (in colorbar) as a function of the cut ℓ_A; for $L = 100$, and $W = 1.0$. (e) Entanglement entropy growth for the first half of the cuts corresponding to (d).

the same constant, $S_\infty/L \approx \frac{1}{4}\ln 2$, as is shown in the inset of Fig. 2(b). This value is considerably smaller than the Page value $S_{\text{Page}} = \frac{1}{2}L\ln 2 - \frac{1}{2}$ [48], contrary to the case of coupling to noise in *interacting* systems [49]. Since in our case the state of the system is a product state for all times, though not necessarily in the position basis, the saturation value better agrees with the entanglement entropy density averaged over all possible product states, given by $\bar{\mathcal{S}}/L \approx 0.193$ (see Eq. (2) in Ref. [50]), and not over all possible states in the entire Hilbert space, which would correspond to the Page value. Before concluding this section, it is worthwhile to observe that the entire behavior of the averaged entanglement entropy in Fig. 2 is somewhat reminiscent of the entanglement entropy behavior in many-body localized systems [51, 52], though, as we will see in what follows, here the system is delocalized by the noise, which induces a slow particle transport.

In order to assess how the entanglement spreads spatially, we compute the averaged entanglement entropy for various cuts through the system. Fig. 2(d), shows the entanglement profile at all times for different cuts (sizes) of the subsytem A, ℓ_A. Analogously, panel (e) shows the time evolution of the entanglement entropy in lines as a function of ℓ_A. It is clear that the delay in the logarithmic entanglement growth is proportional to the distance from the cut to the noise term located at the middle of the chain, $|L/2 - \ell_A|$. The logarithmic growth starts showing up at earlier times as the cut becomes closer to the noise term, while for cuts $\ell_A \ll L/2$ no growth can be observed in the time window explored. As we discussed above, since the spreading of entanglement entropy is an upper bound for other forms of correlations, we expect that any other dynamical behavior in the system to scale at most logarithmically with time.

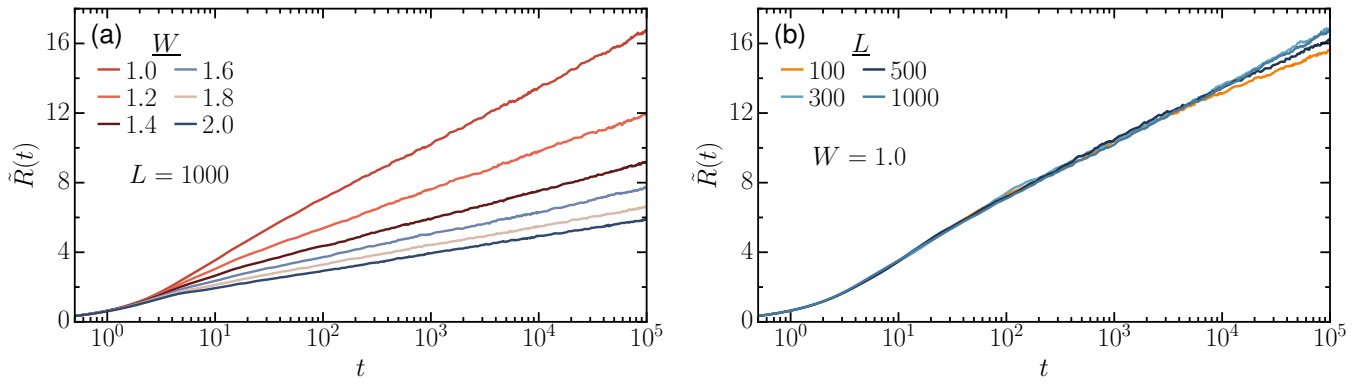

Figure 3. RMS displacement $\tilde{R}(t)$ as a function of time showing logarithmic transport in the system. (a) For various disorder strengths W and $L = 1000$, and (b) for various system sizes L and $W = 1.0$.

C. Particle transport at infinite temperature

In the previous subsections we have studied the approach of the system to the infinite-temperature state. Here, we consider particle transport at infinite temperature. Since in the absence of noise, all single-particle states are localized, there is no transport, even at infinite temperature. Therefore, all transport is induced by the local noise. To assess particle transport we compute the density-density correlation function

$$C_{ij}(t) = \mathrm{Tr}\left(\hat{\rho}_\infty \hat{n}_i(t)\hat{n}_j\right) = \left|\mathrm{Tr}\left(\hat{\rho}_\infty \hat{c}_i^\dagger(t)\hat{c}_j\right)\right|^2, \tag{16}$$

which corresponds to the spreading of an excitation of the density at site j. The last equality follows from the fact that the particles are noninteracting, and $\hat{\rho}_\infty \propto \mathbb{1}$. For the unitary unraveling of (4) that we use here, the evolution of $\hat{c}_i^\dagger(t)$ is given by $\hat{c}_i^\dagger(t) = \sum_k U_{ik}^s(t,0)\hat{c}_k^\dagger$, therefore,

$$C_{ij}(t) = \left|\sum_k U_{ik}^s(t,0)\rho_{kj}^s\right|^2 = \frac{1}{4}\left|U_{ij}^s(t,0)\right|^2, \tag{17}$$

where we used the infinite-temperature form of the single-particle density matrix, $\rho_{kl}^s = \frac{1}{2}\delta_{kl}$. To characterize the nature of transport in the presence of the local noise, we first evaluate the width of the excitation profile, known as the root-mean-square (RMS) displacement,

$$\tilde{R}(t) = \left(\sum_{i=1}^{L}(i-j)^2\left[\overline{C_{ij}(t)}\right]\right)^{1/2}. \tag{18}$$

For diffusive transport, $\tilde{R}(t) \sim \sqrt{2Dt}$, where D is the linear response diffusion constant [53, 54], and for localization the width is bounded, $\tilde{R}(t) \leq A$.

In Ref. [26], it was shown that the Anderson insulator subject to *global* noise with arbitrary correlation time exhibits transient subdiffusion, before asymptotic diffusion takes place. In contrast, in the case of local white noise, we find that the RMS displacement $\tilde{R}(t)$ grows logarithmically with time, without any signs of crossover to diffusion (see Fig. 3(a)). Similarly to the energy and the entanglement entropy, transport is suppressed with increasing the disorder strength. In Fig. (3)(b) we show that our results do not suffer from finite-size effects over a broad time window spanning several decades.

IV. SEMI-ANALYTICAL PICTURE

In this section we provide a theoretical model of nonequilibrium dynamics in the Anderson insulator in the presence of a local noise, which gives a qualitative explanation of the phenomenology we observe. For this purpose we use a variable-range-hopping-like approach, as originally introduced by Mott in the context of phonons [18]. In this

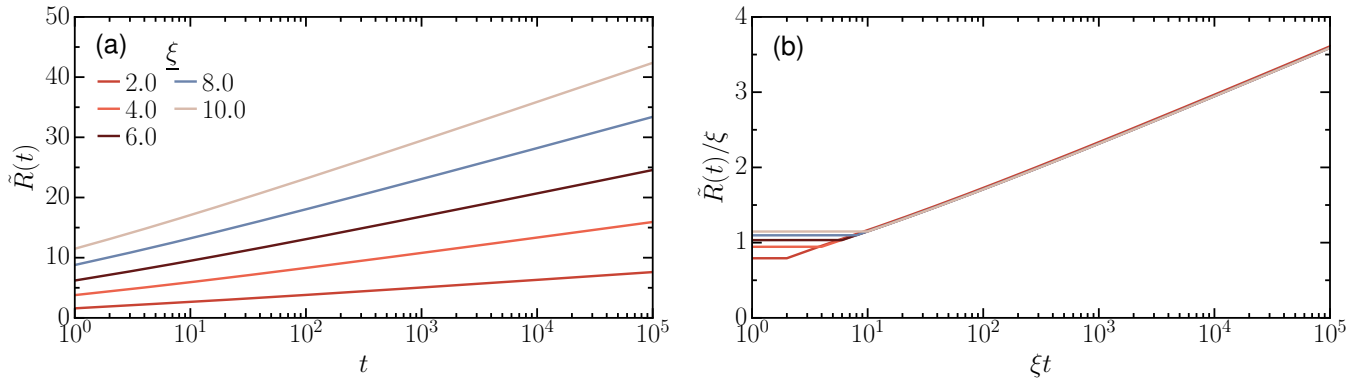

Figure 4. Logarithmic RMS displacement $\tilde{R}(t)$ as a function of time corresponding to the analytical picture. (a) For various localization lengths ξ and $L = 1000$. (b) The same as (a), but $\tilde{R}(t)/\xi$ plotted vs ξt.

approach, the environment induces hopping between the localized orbitals of the Anderson problem. Moreover, it is assumed that the noise decoheres the dynamics, such that the process can be described by a classical master equation [22, 23, 55],

$$\partial_t p_\alpha = \sum_\beta \left(\Gamma_{\alpha\beta} p_\beta - \Gamma_{\beta\alpha} p_\alpha\right), \tag{19}$$

where p_α is the probability to find a particle at an Anderson eigenstate $\langle i|\,\alpha\rangle = \phi_\alpha(i)$, and

$$\begin{aligned}\Gamma_{\alpha\beta} = \Gamma_{\beta\alpha} &= \gamma^2 \left|\langle\beta|\,L/2\rangle\,\langle L/2|\,\alpha\rangle\right|^2 \\ &= \gamma^2 \left|\phi^*_\beta\left(\frac{L}{2}\right)\phi_\alpha\left(\frac{L}{2}\right)\right|^2,\end{aligned} \tag{20}$$

are the transition rates between Anderson eigenstates $|\alpha\rangle$ and $|\beta\rangle$, where to obtain the rates we used the noise coupling $\gamma\,|L/2\rangle\,\langle L/2|$, and the fact that the noise is white. Since the Anderson eigenstates are localized, in a one-dimensional lattice the indices α can be ordered almost in one-to-one correspondence with the site indices i, thus we can write,

$$\Gamma_{\alpha\beta} = \gamma^2 e^{-|\alpha - L/2|/\xi} e^{-|\beta - L/2|/\xi}, \tag{21}$$

where ξ is the localization length. We see that the transition rates between a pair of states are exponentially suppressed with the distance from the local noise, which explains the exponentially long-time scales we observe. To see this more precisely, we numerically solve (19) for a particle initially located at the center of the lattice. In this case the RMS displacement is given by $\tilde{R}(t) = \sqrt{\sum_\alpha \left(\alpha - \frac{L}{2}\right)^2 p_\alpha(t)}$, and is plotted in Fig. 4(a) for various localization lengths, ξ. Plotting $\tilde{R}(t)/\xi$ with respect to ξt results in a perfect collapse of the data, as shown in Fig. 4(b), indicating that the RMS displacement scales as $\tilde{R}(t) \sim \xi \ln(\xi t)$, which is in excellent agreement with the quantum simulation in the previous section, though we could not produce a similar collapse for the original problem (2) with ξ computed numerically. This might indicate that more than one scaling parameter might be required.

V. DISCUSSION

We have studied the dynamical behavior of the Anderson insulator in the presence of a local noisy potential. While the dynamics is dissipative, it can be efficiently studied using an ensemble of pure states, which evolve under *unitary* evolution [42, 43]. Physically, this corresponds to dynamics in the presence of a local, time-dependent potential with a very wide bandwidth of frequencies, which allows us to consider, in addition to the energy absorption, the growth of the entanglement entropy. We find that both quantities grow logarithmically in time and saturate after times that diverge exponentially with system size. While the local noise leads to an infinite-temperature state at long times, the entanglement entropy saturates to an extensive value which is smaller than the Page value [48], but that is in good agreement with the average entanglement entropy over all product states [50]. Interestingly, the entanglement

entropy growth we observe is similar to that of many-body localized systems [51, 52], but contrary to MBL systems, the local noise induces slow logarithmic particle transport at infinite temperature. This scenario is also different from the case of global coupling to noise, where subdiffusive transport is only a transient and asymptotically the system is diffusive [26]. While in this work we have studied a one-dimensional Anderson insulator, the analytical picture we have presented suggests that our results should hold as long as there are no delocalized single-particle states.

We show that the slow dynamical behavior of the Anderson insulator in the presence of a local noise, can be qualitatively understood using a classical master equation, which describes noise-mediated hopping of a particle between localized single-particle states, similar to the variable-range-hopping mechanism [18, 22, 23, 55]. In particular, we show that the RMS displacement of the particle grows as, $\tilde{R}(t) \sim \xi \ln \xi t$, indicating a vanishing diffusion coefficient. Based on this analysis, it is easy to see that our results should hold for any noise which operates in a bounded spatial region, however, the system will become delocalized if the noise operates on a finite fraction of the lattice, p. In this case, the average distance between the noisy sites would be $\ell = 1/p$, and the system would delocalize in a time scale, $t \sim \xi^{-1} \exp[\ell/\xi]$, exhibiting diffusive transport [26, 34]. Our results provide an upper bound for the delocalization rate of Anderson and MBL systems in the presence of local ergodic grains, discussed in Refs. [56, 57], since unlike the grains, the local noise does not "cool down". Our predictions could be feasibly assessed in quantum simulators with ultracold atoms.

We thank Lev Vidmar for bringing to our attention Ref. [50], where the average entanglement entropy over all possible product states is obtained analytically. This research was supported by a grant from the United States-Israel Binational Foundation (BSF, Grant No. 2019644), Jerusalem, Israel, and the United States National Science Foundation (NSF, Grant No. DMR-1936006), and by the Israel Science Foundation (grants No. 527/19 and 218/19). TLML acknowledges funding from the Kreitman fellowship.

[1] P. W. Anderson, Absence of diffusion in certain random lattices, Phys. Rev. **109**, 1492 (1958)
[2] P. A. Lee and T. V. Ramakrishnan, Disordered electronic systems, Rev. Mod. Phys. **57**, 287 (1985)
[3] B. Kramer and A. MacKinnon, Localization: theory and experiment, Rep. Prog. Phys. **56**, 1469 (1993)
[4] L. Fleishman and P. W. Anderson, Interactions and the anderson transition, Phys. Rev. B **21**, 2366 (1980)
[5] D. Basko, I. Aleiner, and B. Altshuler, Metal-insulator transition in a weakly interacting many-electron system with localized single-particle states, Ann. Phys. (N. Y.) **321**, 1126 (2006)
[6] I. V. Gornyi, A. D. Mirlin, and D. G. Polyakov, Interacting Electrons in Disordered Wires: Anderson Localization and Low-T Transport, Phys. Rev. Lett. **95**, 206603 (2005)
[7] E. Abrahams, P. W. Anderson, D. C. Licciardello, and T. V. Ramakrishnan, Scaling theory of localization: Absence of quantum diffusion in two dimensions, Phys. Rev. Lett. **42**, 673 (1979)
[8] A. D. Mirlin, Statistics of energy levels and eigenfunctions in disordered systems, Phys. Rep. **326**, 259 (2000)
[9] F. Evers and A. D. Mirlin, Anderson transitions, Rev. Mod. Phys. **80**, 1355 (2008)
[10] C. A. Condat and T. R. Kirkpatrick, Observability of acoustical and optical localization, Phys. Rev. Lett. **58**, 226 (1987)
[11] D. S. Wiersma, P. Bartolini, A. Lagendijk, and R. Righini, Localization of light in a disordered medium, Nature **390**, 671 (1997)
[12] J. Billy, V. Josse, Z. Zuo, A. Bernard, B. Hambrecht, P. Lugan, D. Clément, L. Sanchez-Palencia, P. Bouyer, and A. Aspect, Direct observation of anderson localization of matter waves in a controlled disorder, Nature **453**, 891 (2008)
[13] G. Roati, C. D'Errico, L. Fallani, M. Fattori, C. Fort, M. Zaccanti, G. Modugno, M. Modugno, and M. Inguscio, Anderson localization of a non-interacting bose-einstein condensate, Nature **453**, 895 (2008)
[14] L. Sanchez-Palencia and M. Lewenstein, Disordered quantum gases under control, Nat. Phys. **6**, 87 (2010)
[15] S. Kondov, W. McGehee, J. Zirbel, and B. DeMarco, Three-dimensional anderson localization of ultracold matter, Science **334**, 66 (2011)
[16] F. Jendrzejewski, A. Bernard, K. Mueller, P. Cheinet, V. Josse, M. Piraud, L. Pezzé, L. Sanchez-Palencia, A. Aspect, and P. Bouyer, Three-dimensional localization of ultracold atoms in an optical disordered potential, Nat. Phys. **8**, 398 (2012)
[17] M. Segev, Y. Silberberg, and D. N. Christodoulides, Anderson localization of light, Nature Photonics **7**, 197 (2013)
[18] N. Mott, Conduction in non-crystalline materials, Philos. Mag. **19**, 835 (1969)
[19] B. L. Altshuler, Y. Gefen, A. Kamenev, and L. S. Levitov, Quasiparticle lifetime in a finite system: A nonperturbative approach, Phys. Rev. Lett. **78**, 2803 (1997)
[20] J. Bourgain and W.-M. Wang, Anderson localization for time quasi-periodic random schrödinger and wave equations, Commun. Math. Phys. **248**, 429 (2002)
[21] A. S. Pikovsky and D. L. Shepelyansky, Destruction of anderson localization by a weak nonlinearity, Phys. Rev. Lett. **100**, 094101 (2008)
[22] A. Amir, Y. Lahini, and H. B. Perets, Classical diffusion of a quantum particle in a noisy environment, Phys. Rev. E **79**, 050105 (2009)
[23] A. Amir, Y. Oreg, and Y. Imry, Localization, anomalous diffusion, and slow relaxations: A random distance matrix

approach, Phys. Rev. Lett. **105**, 070601 (2010)
[24] S. Fishman, Y. Krivolapov, and A. Soffer, The nonlinear schrödinger equation with a random potential: results and puzzles, Nonlinearity **25**, R53 (2012)
[25] D. A. Huse, R. Nandkishore, F. Pietracaprina, V. Ros, and A. Scardicchio, Localized systems coupled to small baths: From anderson to zeno, Phys. Rev. B **92**, 014203 (2015)
[26] S. Gopalakrishnan, K. R. Islam, and M. Knap, Noise-induced subdiffusion in strongly localized quantum systems, Phys. Rev. Lett. **119**, 046601 (2017)
[27] F. Huveneers and R. Ducatez, Anderson localization for periodically driven systems, Ann. Henri Poincare , 2415 (2017)
[28] S. Lorenzo, T. Apollaro, G. M. Palma, R. Nandkishore, A. Silva, and J. Marino, Remnants of anderson localization in prethermalization induced by white noise, Phys. Rev. B **98**, 054302 (2018)
[29] K. Agarwal, S. Ganeshan, and R. N. Bhatt, Localization and transport in a strongly driven anderson insulator, Phys. Rev. B **96**, 014201 (2017)
[30] Y. Gefen and G. Schön, Effect of inelastic processes on localization in one dimension, Phys. Rev. B **30**, 7323 (1984)
[31] D. E. Logan and P. G. Wolynes, Dephasing and anderson localization in topologically disordered systems, Phys. Rev. B **36**, 4135 (1987)
[32] D. Evensky, R. Scalettar, and P. G. Wolynes, Localization and dephasing effects in a time-dependent anderson hamiltonian, J. Phys. Chem. **94**, 1149 (1990)
[33] D. Evensky and P. G. Wolynes, Transport of dipolar excitons in disordered systems, Chem. Phys. Lett. **209**, 185 (1993)
[34] S. R. Taylor and A. Scardicchio, Subdiffusion in a one-dimensional anderson insulator with random dephasing: Finite-size scaling, griffiths effects, and possible implications for many-body localization, Phys. Rev. B **103**, 184202 (2021)
[35] M. Schreiber, S. S. Hodgman, P. Bordia, H. P. Lüschen, M. H. Fischer, R. Vosk, E. Altman, U. Schneider, and I. Bloch, Observation of many-body localization of interacting fermions in a quasirandom optical lattice, Science **349**, 842 (2015)
[36] P. Bordia, H. P. Lüschen, S. S. Hodgman, M. Schreiber, I. Bloch, and U. Schneider, Coupling identical one-dimensional many-body localized systems, Phys. Rev. Lett. **116**, 140401 (2016)
[37] H. P. Lüschen, P. Bordia, S. S. Hodgman, M. Schreiber, S. Sarkar, A. J. Daley, M. H. Fischer, E. Altman, I. Bloch, and U. Schneider, Signatures of many-body localization in a controlled open quantum system, Phys. Rev. X **7**, 011034 (2017)
[38] G. Lindblad, On the generators of quantum dynamical semigroups, Commun. Math. Phys. **48**, 119 (1976)
[39] M. B. Plenio and P. L. Knight, The quantum-jump approach to dissipative dynamics in quantum optics, Rev. Mod. Phys. **70**, 101 (1998)
[40] C. Gardiner and P. Zoller, *Quantum noise: a handbook of Markovian and non-Markovian quantum stochastic methods with applications to quantum optics* (Springer Science & Business Media, 2004)
[41] T. A. Brun, Continuous measurements, quantum trajectories, and decoherent histories, Phys. Rev. A **61**, 042107 (2000)
[42] H. M. Wiseman and L. Diósi, Complete parameterization, and invariance, of diffusive quantum trajectories for markovian open systems, Chem. Phys. **268**, 91 (2001)
[43] D. Salgado and J. Sánchez-Gómez, Expressing stochastic unravellings using random evolution operators, J. Opt. B Quantum Semiclassical Opt. **4**, S458 (2002)
[44] J. Rehn, A. Lazarides, F. Pollmann, and R. Moessner, How periodic driving heats a disordered quantum spin chain, Phys. Rev. B **94**, 020201 (2016)
[45] J. Eisert and M. Plenio, Introduction to the basics of entanglement theory in continuous-variable systems, Int. J. Quantum Inf. **01**, 479 (2003)
[46] X. Cao, A. Tilloy, and A. De Luca, Entanglement in a fermion chain under continuous monitoring, SciPost Phys. **7**, 24 (2019)
[47] I. Peschel and V. Eisler, Reduced density matrices and entanglement entropy in free lattice models, J. Phys. A **42**, 504003 (2009)
[48] D. N. Page, Average entropy of a subsystem, Phys. Rev. Lett. **71**, 1291 (1993)
[49] E. Levi, M. Heyl, I. Lesanovsky, and J. P. Garrahan, Robustness of many-body localization in the presence of dissipation, Phys. Rev. Lett. **116**, 237203 (2016)
[50] P. Łydżba, M. Rigol, and L. Vidmar, Eigenstate entanglement entropy in random quadratic hamiltonians, Phys. Rev. Lett. **125**, 180604 (2020)
[51] M. Žnidarič, T. Prosen, and P. Prelovšek, Many-body localization in the heisenberg xxz magnet in a random field, Phys. Rev. B **77**, 064426 (2008)
[52] J. H. Bardarson, F. Pollmann, and J. E. Moore, Unbounded growth of entanglement in models of many-body localization, Phys. Rev. Lett. **109**, 017202 (2012)
[53] R. Steinigeweg, H. Wichterich, and J. Gemmer, Density dynamics from current auto-correlations at finite time- and length-scales, EPL **88**, 10004 (2009)
[54] R. Steinigeweg, F. Jin, D. Schmidtke, H. De Raedt, K. Michielsen, and J. Gemmer, Real-time broadening of nonequilibrium density profiles and the role of the specific initial-state realization, Phys. Rev. B **95**, 035155 (2017)
[55] M. H. Fischer, M. Maksymenko, and E. Altman, Dynamics of a many-body-localized system coupled to a bath, Phys. Rev. Lett. **116**, 160401 (2016)
[56] D. J. Luitz, F. m. c. Huveneers, and W. De Roeck, How a small quantum bath can thermalize long localized chains, Phys. Rev. Lett. **119**, 150602 (2017)
[57] V. Khemani, S. P. Lim, D. N. Sheng, and D. A. Huse, Critical properties of the many-body localization transition, Phys. Rev. X **7**, 021013 (2017)